Available online at www.sciencedirect.com
SCIENCE DIRECT®
Environmental Pollution 133 (2005) 351–364
ENVIRONMENTAL POLLUTION
www.elsevier.com/locate/envpol

Modelling the transport of suspended particulate matter by the Rhone River plume (France). Implications for pollutant dispersion

R. Periáñez*

Departamento Física Aplicada I, E.U. Ingeniería Técnica Agrícola, Universidad de Sevilla. Ctra. Utrera km 1, 41013-Sevilla, Spain

Received 25 January 2004; accepted 21 May 2004

A model has been developed to simulate transport of suspended particulate matter in the Rhone River plume.

Abstract

A model to simulate the transport of suspended particulate matter by the Rhone River plume has been developed. The model solves the 3D hydrodynamic equations, including baroclinic terms and a 1-equation turbulence model, and the suspended matter equations including advection/diffusion of particles, settling and deposition. Four particle classes are considered simultaneously according to observations in the Rhone. Computed currents, salinity and particle distributions are, in general, in good agreement with observations or previous calculations. The model also provides sedimentation rates and the distribution of different particle classes over the sea bed. It has been found that high sedimentation rates close to the river mouth are due to coarse particles that sink rapidly. Computed sedimentation rates are also similar to those derived from observations. The model has been applied to simulate the transport of radionuclides by the plume, since suspended matter is the main vector for them. The radionuclide transport model, previously described and validated, includes exchanges of radionuclides between water, suspended matter and bottom sediment described in terms of kinetic rates. A new feature is the explicit inclusion of the dependence of kinetic rates upon salinity. The model has been applied to ^{137}Cs and ^{239,240}Pu. Results are, in general, in good agreement with observations.

Keywords: Rhone River; Numerical modelling; Suspended matter; Sediments; Hydrodynamics; Dispersion; Cesium; Plutonium

1. Introduction

In recent years there has been an increasing interest in modelling suspended matter since this is essential for water quality models. First, when sediment is stirred up nutrients, trace metals and organic contaminants are released into the water column. In turn, as suspended sediment settles out the dissolved chemicals may be scavenged. Secondly, since the light intensity at depth depends inversely on suspended sediment load in the water column above, suspended matter impacts on primary productivity (Morris and Howarth, 1998). Thus, mathematical models have been developed to simulate the suspended matter distributions in different aquatic environments and under different approaches, from relatively simple box models (Puls and Sundermann, 1990; Abril and García-León, 1994) to more complex dynamic approaches in which advection, diffusion and settling of particles are computed from calculated current fields (for instance Clarke and Elliott, 1998; Cancino and Neves, 1999; Periáñez, 2002; Lumborg and Windelin, 2003).

* Tel.: +34 954 486 474; fax: +34 954 486 436.
E-mail address: rperianez@us.es.

0269-7491/$ - see front matter © 2004 Elsevier Ltd. All rights reserved.
doi:10.1016/j.envpol.2004.05.021

By convention, particulate matter in suspension is defined as the material that is retained on a 0.4–0.5 μm pore size filter. Smaller material is considered to be dissolved. Muddy sediments consist of clays with some variable silt content and particle diameter (Pugh, 1987) is <62.5 μm. Larger particles such as sands settle much more rapidly out of suspension in water than mud particles and bed load transport is the most important mechanism in moving these coarse sediments (Pugh, 1987; Morris and Howarth, 1998). Usually, only particles with diameters <62.5 μm are considered when modelling suspended matter dynamics (see for instance Clarke, 1995; Nicholson and O'Connor, 1986; Periáñez et al., 1996; Periáñez, 2002). Indeed, it has been pointed out (Eisma, 1981) that for all practical purposes mud can be regarded synonymous of suspended matter. Also, contaminants have little affinity for coarse materials and, on the other hand, they have little influence on light intensity through the water column since they are mainly transported as bed load. Thus, the dynamics of muddy sediments is much more interesting for water quality studies.

The objective of this paper consists of presenting a suspended matter model to simulate the transport of sediments by the Rhone River plume, in the western Mediterranean Sea. This is an interesting problem since a complex intrusion process occurs when a freshwater input runs into marine waters. It mainly depends upon the interaction between the bouyancy induced momentum fluxes, which spread the freshwater offshore, and the turbulent dilution and dissipation mechanisms, which reduce density differences between the two water masses. For the Rhone, a thin upper layer (2 m), forming a well-identified surface plume, is separated from ambient seawater by a sharp transition where the salinity exhibits a jump of 10 or 20 g/L and extends offshore over distances of the order of 20 or 30 km (Broche et al., 1998). The model solves the three-dimensional hydrodynamic equations, including baroclinic terms and a 1-equation turbulence model, and the suspended matter equations. These include advection/diffusion, settling and deposition of particles on the sea bed. Four particle classes are considered simultaneously. The model also provides sedimentation rates, that can be compared with those derived from observations, and the distribution of particles of different classes over the sea bed. It must be pointed out that some detailed models have already been developed to study the water circulation in the Rhone plume (Estournel et al., 1997; Marsaleix et al., 1998; Estournel et al., 2001). Also, some models describe the transport of sediments in the plume (Kondrachoff et al., 1994; Estournel et al., 1997), although in a rather simple way. Indeed, only one particle size was considered in these references and deposition was not included. Thus, they merely focused on reproducing the shape of the surface plume.

Artificial radionuclides have been released to the Rhone River mainly from Marcoule nuclear fuel reprocessing plant. These radionuclides are transported downstream until they are introduced into the Mediterranean by the river plume. It has been found (Martin and Thomas, 1990) that the particulate phase is the major vector for most of the radionuclides. Thus, an accurate suspended matter model is required to properly simulate the dispersion of radionuclides in the plume. The suspended particulate model has been coupled to a radionuclide model to simulate the dispersion of ^{137}Cs and ^{239,240}Pu, radionuclides with different geochemical behaviours. The radionuclide dispersion model includes advection/diffusion processes and the transfers between the liquid and solid phases (suspended matter and bottom sediments), which are described in terms of kinetic transfer coefficients. This radionuclide dispersion model has been previously applied to marine and estuarine environments, but it has not been used before for a river plume. A new feature of the model is, however, the inclusion of the explicit dependence of kinetic coefficients upon water salinity. Model results for radionuclide distributions are, in general, in good agreement with observations, which provides an extra validation of the suspended matter model. Models for simulating the dispersion of contaminants by the Rhone plume have not been previously developed.

The suspended matter model is presented in the following section. Next, results for suspended particles and radionuclides are described and discussed.

2. Description of the model

2.1. Hydrodynamic model

The full 3D hydrodynamic equations including the terms corresponding to density gradients can be written in the hydrostatic and Boussinesq approximations as (Kowalick and Murty, 1993):

$$\frac{\partial \zeta}{\partial t}+\frac{\partial}{\partial x}\left[(h+\zeta)\int_{-h}^{\zeta} u\,\mathrm{d}z\right]+\frac{\partial}{\partial y}\left[(h+\zeta)\int_{-h}^{\zeta} v\,\mathrm{d}z\right]=0 \qquad (1)$$

$$\frac{\partial u}{\partial t}+u\frac{\partial u}{\partial x}+v\frac{\partial u}{\partial y}-\Omega v+g\frac{\partial \zeta}{\partial x}+\frac{g}{\rho_0}\int_{z}^{\zeta}\frac{\partial \rho_w}{\partial x}\mathrm{d}z = \frac{\partial}{\partial z}\left(K\frac{\partial u}{\partial z}\right)+A\left(\frac{\partial^2 u}{\partial x^2}+\frac{\partial^2 u}{\partial y^2}\right) \qquad (2)$$

$$\frac{\partial v}{\partial t}+u\frac{\partial v}{\partial x}+v\frac{\partial v}{\partial y}+\Omega u+g\frac{\partial \zeta}{\partial y}+\frac{g}{\rho_0}\int_z^{\zeta}\frac{\partial \rho_w}{\partial y}dz$$
$$=\frac{\partial}{\partial z}\left(K\frac{\partial v}{\partial z}\right)+A\left(\frac{\partial^2 v}{\partial x^2}+\frac{\partial^2 v}{\partial y^2}\right) \quad (3)$$

where the z coordinate is measured upwards from the undisturbed sea level, h is water depth, ζ is the displacement of the sea surface from the undisturbed level, u and v are the two components of the water velocity along the x and y axis, respectively, Ω is the Coriolis parameter, ρ_w is water density, ρ_0 is a reference density, and K and A are the vertical and horizontal eddy viscosities, respectively.

The vertical component of the water velocity, w, is obtained from the continuity equation:

$$\frac{\partial u}{\partial x}+\frac{\partial v}{\partial y}+\frac{\partial w}{\partial z}=0 \quad (4)$$

The water density is derived from an equation of state relating density to salinity (Kowalick and Murty, 1993):

$$\rho_w=\rho_0(1+\alpha S) \quad (5)$$

where S is salinity and $\alpha = 7.45\times10^{-4}$. As in Marsaleix et al. (1998), the effect of temperature on density is omitted for the sake of simplicity. Indeed, temperature differences between the Rhone River and the ambient seawater are small enough to consider that the buoyancy effects in the plume are represented only by the salinity gradients (Marsaleix et al., 1998). The reference salinity is taken as $\rho_0 = 998.9$ kg/m^3.

The salinity is determined from an advection–diffusion equation:

$$\frac{\partial S}{\partial t}+u\frac{\partial S}{\partial x}+v\frac{\partial S}{\partial y}+w\frac{\partial S}{\partial z}=A\left(\frac{\partial^2 S}{\partial x^2}+\frac{\partial^2 S}{\partial y^2}\right)+\frac{\partial}{\partial z}\left(K\frac{\partial S}{\partial z}\right) \quad (6)$$

Vertical eddy viscosity is determined from the 1-equation turbulence model described in Davies and Hall (2000). This model has also been used in Xing and Davies (1999) to simulate a river plume. The equation for the turbulent kinetic energy E is:

$$\frac{\partial E}{\partial t}=K\left\{\left(\frac{\partial u}{\partial z}\right)^2+\left(\frac{\partial v}{\partial z}\right)^2\right\}+\beta_0\frac{\partial}{\partial z}\left(K\frac{\partial E}{\partial z}\right)-\varepsilon+\frac{g}{\rho_0}K\frac{\partial \rho}{\partial z} \quad (7)$$

The first term in the right side of the equation represents generation of turbulence by the vertical shear, the second term is diffusion of turbulence and the last term is loss of turbulence by buoyancy (conversion of kinetic energy into potential energy). ε represents turbulence dissipation that is written as:

$$\varepsilon=C_1E^{3/2}\ell \quad (8)$$

where ℓ is a mixing length and C_1 a numeric coefficient. The vertical viscosity is finally written as a function of energy as:

$$K=C_0\ell E^{1/2}+\lambda_t \quad (9)$$

where C_0 is a numeric coefficient and λ_t is a background value of viscosity, that is the minimum possible value that it may have (Ruddick et al., 1995; Cugier and Le Hir, 2002). The values given to the numeric constants appearing above are (Davies and Hall, 2000): $\beta_0 = 0.73$, $C_0 = C^{1/4}$, $C_1 = {C_0}^3$ and $C = 0.046$. The background viscosity is fixed as $\lambda_t = 10^{-4}$ m^2/s, which is the same value used in Ruddick et al. (1995).

The mixing length is derived from an algebraic expression (Davies and Hall, 2000):

$$\ell=\frac{1}{1/\ell_1+1/\ell_2} \quad (10)$$

with

$$\ell_1=\kappa(z+z_0+h)\exp\left(\beta_1\frac{z+h}{h}\right) \quad (11)$$

$$\ell_2=\kappa(z_s-z) \quad (12)$$

where $\kappa = 0.4$ is the von Karman's constant, $\beta_1 = -2.0$ and z_s and z_0 are the roughness lengths of the sea surface and bottom, respectively.

Boundary conditions have also to be provided for sea surface elevation, currents, salinity and kinetic energy. At the sea surface and bottom there is no flux of salinity. At the surface, the internal stress is set equal to the external wind stress and at the bottom a quadratic friction law is applied.

In the case of kinetic energy, the boundary condition at the sea surface is:

$$E_{z=\zeta}=\frac{\tau_w}{\rho_0\sqrt{C_E}} \quad (13)$$

where τ_w is the wind stress and $C_E = 0.07$ (Estournel et al., 1997). If there is no wind, the flux of energy at the surface is set to zero. At the sea bottom, boundary condition is:

$$E_{z=-h}=\frac{\tau_b}{\rho_0\sqrt{C_E}} \quad (14)$$

where τ_b is the bottom stress and $C_E = 0.07$ as in Estournel et al. (1997).

A no-flux condition is applied along land boundaries. A radiation condition in the form of Orlanski (1976) is applied along open boundaries for the water velocity component that is normal to the boundary:

$$\frac{\partial \xi}{\partial t} + c\frac{\partial \xi}{\partial n} = 0 \tag{15}$$

where n is the direction normal to the boundary, $\xi = u,v$ is the water velocity component to which the condition is applied and c is the wave speed calculated as in Orlanski (1976). This condition has also been used in Marsaleix et al. (1998). Surface elevations should be prescribed along open boundaries to propagate tides inside the computational domain. However, as will be shown below, tides can be neglected in the present model application and a radiation condition will also be applied to determine water surface elevations along open boundaries.

Boundary conditions at the river mouth are:

$$S = 0 \tag{16}$$

that is the freshwater value and

$$q_l = \frac{Q}{ld} \tag{17}$$

where q_l is the water velocity in the direction of the outflow, Q is the river discharge and l and d are the width of the river mouth and the thickness of the outflow water layer, respectively.

2.2. Suspended sediment model

The suspended sediment dynamic is governed by an advection–diffusion dispersion equation to which the settling, erosion and deposition terms are added. A number, N, of particle classes are considered in the model. Each particle class is represented by a concentration m_i. The equation for size i is:

$$\frac{\partial m_i}{\partial t} + u\frac{\partial m_i}{\partial x} + v\frac{\partial m_i}{\partial y} + (w - w_{s,i})\frac{\partial m_i}{\partial z} = A\left(\frac{\partial^2 m_i}{\partial x^2} + \frac{\partial^2 m_i}{\partial y^2}\right) + \frac{\partial}{\partial z}\left(K\frac{\partial m_i}{\partial z}\right) \tag{18}$$

where $w_{s,i}$ is the corresponding settling velocity for particle class i. The deposition and erosion terms are incorporated into the sea bed boundary condition of the equation. The deposition rate is written as in other modelling studies (see for instance Nicholson and O'Connor, 1986; Holt and James, 1999; Liu et al., 2002a; Lumborg and Windelin, 2003; Wu et al., 1998; Prandle et al., 2000; Cancino and Neves, 1999):

$$\mathrm{DP}_i = w_{s,i} m_i(b)\left(1 - \frac{\tau_b}{\tau_{cd}}\right) \tag{19}$$

where $m_i(b)$ is particle concentration of class i evaluated at the sea bottom and τ_{cd} is a critical deposition stress above which no deposition occurs since particles are maintained in suspension by water turbulence.

The settling velocity for each particle class is determined from Stokes's law:

$$w_{s,i} = \frac{\rho - \rho_w}{\rho_w}\frac{gD_i^2}{18\nu} \tag{20}$$

where ρ and D_i are suspended particle density and diameter, respectively and ν is kinematic viscosity of water. It is also possible to include the process of aggregation in the model through a classic relationship in the form (Mehta, 1989; Clarke, 1995):

$$w_{s,i} = a_1 m_i^{a_2} \tag{21}$$

This approach has been used in some suspended sediment models (Cancino and Neves, 1999; Clarke and Elliott, 1998; Nicholson and O'Connor, 1986; Lumborg and Windelin, 2003) and also in radionuclide dispersion models (Periáñez, 1999, 2000). Other authors (Estournel et al., 1997; Liu et al., 2002a, 2002b; Jiang et al., 2000; Segschneider and Sundermann, 1998; Holt and James, 1999) directly calculate the settling velocity from Stokes's law. Tattersall et al. (2003) have used a mixed approach. At each time step the settling velocity resulting from Eq. (21) is calculated and compared with that obtained from Stokes's law. Then the higher value is used. Wu et al. (1998) use Eq. (21) or Stokes's law depending on the suspended matter concentration. Stokes's law has been used in this work due to the difficulty of finding appropriate values for a_1 and a_2 for each particle class. Moreover, Thill et al. (2001) have found that it is not clear that the aggregation process could play a role in enhancing settling at the Rhone River mouth.

The erosion rate is written in terms of the erodability constant (Liu et al., 2002a, 2002b; Cancino and Neves, 1999; Prandle et al., 2000; Holt and James, 1999; Nicholson and O'Connor, 1986):

$$\mathrm{ER}_i = Ef_i\left(\frac{\tau_b}{\tau_{ce}} - 1\right) \tag{22}$$

where E is the erodability constant, f_i gives the fraction of particles of class i in the bed sediment and τ_{ce} is a critical erosion stress below which no erosion occurs. The model can also calculate sedimentation rates as the balance between the deposition and erosion terms.

Bed-load transport of coarse particles has not been included since most contaminants are essentially

adsorbed on the fine particles. This is the case for radionuclides (McKay and Walker, 1990). Such an approach has also been used in other models (for instance Periáñez, 1999).

2.3. Numerical solution

All the equations are solved using explicit finite difference schemes. The scheme described in Flather and Heaps (1975) is used to solve the hydrodynamic equations. For non-linear terms, scheme 2 described in such reference is used. It consists of calculating changes in components of the horizontal current due to advection alone and adding them to the changes caused by other physical processes computed from the hydrodynamic equations without the advective terms. The MSOU second order scheme (Vested et al., 1996) is used to solve the advection terms in all the dispersion equations and a second order scheme (Kowalick and Murty, 1993) is also used for the diffusion terms.

Density gradients are calculated using $\sigma_\theta = \rho_w - 1000$ instead of the density (Kowalick and Murty, 1993). Also, the stability of the water column is checked each time step and over all the model domain. Mixing is carried out, using the algorithm described in Kowalick and Murty (1993), when it becomes unstable. The hydrodynamic calculations are started from rest and a uniform salinity of 38 g/L is assumed. The effect of the large-scale circulation can be neglected in the area under study (Marsaleix et al., 1998), as well as tidal currents, that are practically non-existing (Marsaleix et al., 1998; Tsimplis et al., 1995). Indeed, M_2 currents are below 1 cm/s in most parts of the Mediterranean and S_2 currents have smaller amplitudes.

Open boundary conditions must also be given for suspended matter particles. The open boundary condition described in Periáñez (1999) and Periáñez (2000) has been adopted:

$$C_i = \psi C_{i-1} \tag{23}$$

where C_i represents the concentration of suspended matter and radionuclides along the boundary and C_{i-1} represents the concentration just inside the computational domain. The nondimensional value of ψ is obtained from a calibration exercise.

The hydrodynamic model is run for a given water discharge from the Rhone until a steady salinity and current amplitude pattern is obtained. Then the suspended matter model is run using such water circulation. The suspended matter model (without the erosion term) is started from a sea bottom containing no sediments. Then the accumulation of particles of each class is calculated to have a first estimation of the distribution of sediment particle sizes over the model domain. Next, the suspended matter model is started (with erosion) from the estimated particle class distribution until a steady state is reached. This way a self-consistent distribution of different particle classes on the sea bed over the model domain can be obtained. This distribution is relevant to calculate the adsorption of radionuclides by the bed sediments.

The model domain is presented in Fig. 1. The model resolution is $\Delta x = \Delta y = 1000$ m. A variable grid is used in the vertical to have enough resolution to solve the salinity gradients in the surface plume. Thus, 10 layers with $\Delta z = 1$ m are used followed by thicker layers increasing to $\Delta z = 15$ m. Time step is fixed as 5 s to solve the hydrodynamic equations due to the CFL stability condition. It is increased to 60 s to solve the suspended matter equations.

3. Results

3.1. Model application

Values to the different parameters in the model must be given, as well as the appropriate source term for suspended matter particles. The bed friction coefficient has been fixed as $k = 0.015$ and the horizontal diffusivity as $A = 20\ m^2/s$. The roughness lengths of the sea surface and bottom have been defined as $z_s = z_0 = 0.0034$ m. These values are similar to those used by Xing and Davies (1999). The thickness of the freshwater layer discharged from the Rhone is 2 m (Broche et al., 1998) and the width of the river mouth has been fixed as $d = \Delta x = 1000$ m, which is very close to reality. Indeed, this approach has already been used in Marsaleix et al. (1998). As commented before, large-scale circulation and tides are neglected.

The hydrodynamic model has been run for the average discharge from the Rhone River, $1700\ m^3/s$ (Broche et al., 1998; Thill et al., 2001), and without wind. The computed water circulation and salinity distribution are stored in files that will be used to calculate the suspended matter distribution, deposition rates, the distribution of particles over the sea bed and, finally, the dispersion of radionuclides.

Wind conditions affect the extension and shape of the plume (Estournel et al., 1997, 2001). Two types of winds are predominant in the region: northwest winds (representing 45% of winds exceeding 10 m/s on average over the year) and southeast winds (20% of winds exceeding 10 m/s). The plume response to winds has been studied in the references given above. Although wind stress is formally included in the hydrodynamic equations, the main difficulty in the present work is that observed sedimentation rates, the distribution of different particle classes over the bed and measured radionuclide concentrations in bed sediments integrate many different wind and river discharge conditions. On the

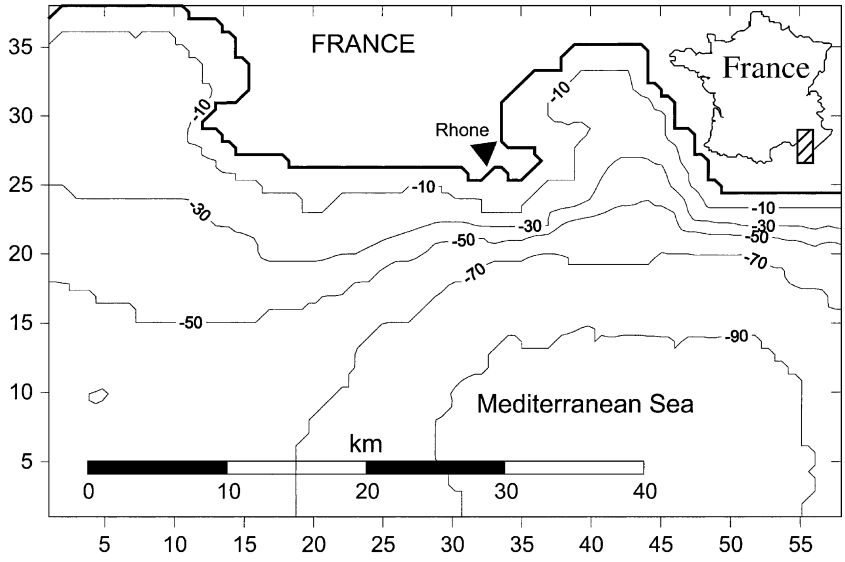

Fig. 1. Model domain. Units in the x and y axis indicate grid cell number. Depths are given in m.

other hand, measured radionuclide concentrations in the water column correspond to the particular conditions during sampling, that, on the other hand, took place over a period of several months (Martin and Thomas, 1990). As a consequence, it was decided to run the hydrodynamic model for average discharge from the Rhone River and without wind. This may be a too simple approach, but can give a realistic view of the main dispersion processes in the plume, given the generally good agreement obtained between computations and measurements. Nevertheless, the sensitivity of radionuclide transport in the plume to changing winds is an interesting problem that has to be addressed in the near future.

The average suspended matter discharge of the Rhone River is about 4.6 Mt/year, which represents the major particle input into the western Mediterranean Sea. However, the solid discharge has a relevant annual variability, with most of the solids being discharged during flood events. Thomas (1997) has established a correlation for the suspended matter concentration in the river vs. water flow. If such correlation is applied to the average water discharge (1700 m^3/s), a suspended matter concentration in the river of 28 mg/L is obtained. This will be the suspended matter source term used in the model. This estimation is in agreement with measurements. For instance, Garnier et al. (1991) measured a suspended load of 17.6 mg/L for a water discharge of 1600 m^3/s; Martin and Thomas (1990) measured 11.3 and 54.0 mg/L for water discharges of 1300 and 2200 m^3/s, respectively and Eyrolle et al. (2002) obtained a suspended load of 28.6 mg/L for a water discharge of 1718 m^3/s.

Four suspended matter particle classes are considered in the model. Thill et al. (2001) measured the proportion of particles of 5 different classes for low, average and high water discharges. From the total particle concentration given above (28 mg/L) and the proportion of particles of each class (for average water discharge), the particle concentration for each class can be calculated. Results are given in Table 1. These concentrations are the boundary conditions of the suspended matter model at the river mouth. The largest particle class has been neglected due to the extremely low proportion in which such particles are present (0.014% of the total). Settling velocities obtained from Stokes's law are also given in Table 1. The threshold deposition stress has been fixed as 0.1 N/m^2. This parameter has been observed to be in the range 0.06–1.1 N/m^2 (Krone, 1962; Mehta and Partheniades, 1975). After some preliminary calculations without wind, it was found that results were not affected by the erosion term. However, erosion events may be induced by wind waves in the shallower areas. Indeed, waves are the main factor producing sediment erosion in the region (REMOTRANS, 2004). Nevertheless, wave-induced erosion is not included in the model since calculations are carried out under calm conditions (the models of Estournel et al. (1997) and Kondrachoff

Table 1
Particle classes included in the model and their corresponding settling velocities

Average particle size (μm)	w_s (m/s)	m (mg/L)
3	7.8×10^{-6}	11.5
7	4.2×10^{-5}	9.5
20	3.5×10^{-4}	3.5
40	1.4×10^{-3}	3.5

Each class is defined by its average particle size. The particle concentration at the Rhone River mouth for average water discharge is also given.

et al. (1994) do not include sediment erosion although they do consider winds). The suspended matter model also provides the distribution of the different particle classes on the sea bed over the model domain (parameter f_i for each class), as well as provides sedimentation rates over the domain, that can be compared with those derived from observations.

3.2. Hydrodynamics and suspended particulate matter

The computed current distribution is in qualitative agreement with the earlier calculations in Estournel et al. (1997), Marsaleix et al. (1998) and Arnoux-Chiavassa (1998). Water discharged by the river moves in a southeast direction and then rotates towards the west due to Coriolis acceleration and moves along the coast. Broche et al. (1998) released a surface drifter 2 km south from the river mouth and measured its langrangian velocity during several hours. The movement of a surface drifter has been simulated with the model for the same conditions of the experiment in Broche et al. (1998), water discharge equal to 2000 m^3/s and no wind. A comparison between the observed and computed langrangian velocity of the drifter is presented in Fig. 2. It can be seen that there is a good agreement between both sets of data, indicating that the model is giving a realistic representation of current magnitudes in the Rhone plume.

The salinity distribution in the surface plume can be seen in the map presented in Fig. 3A. This distribution is essentially the same as that previously computed in Arnoux-Chiavassa (1998), Estournel et al. (1997) and Marsaleix et al. (1998). The shape of the salinity contours, together with the current pattern, indicates that the plume forms a bulge of anticyclonic circulation in front of the river mouth. The circulation in the plume is baroclinic, that is, induced by the density differences.

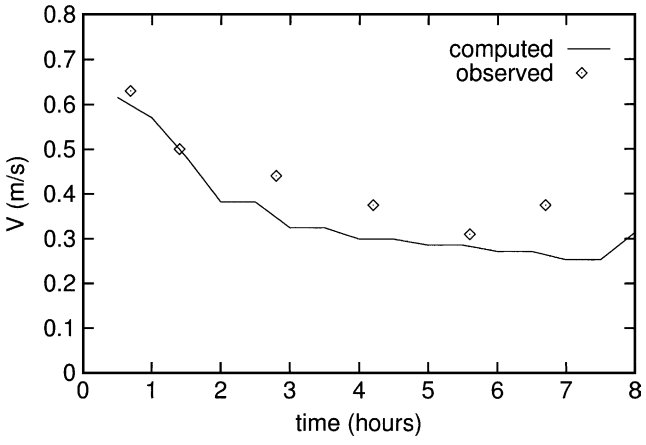

Fig. 2. Observed and computed lagrangian velocities of a surface drifter released 2 km south from the river mouth.

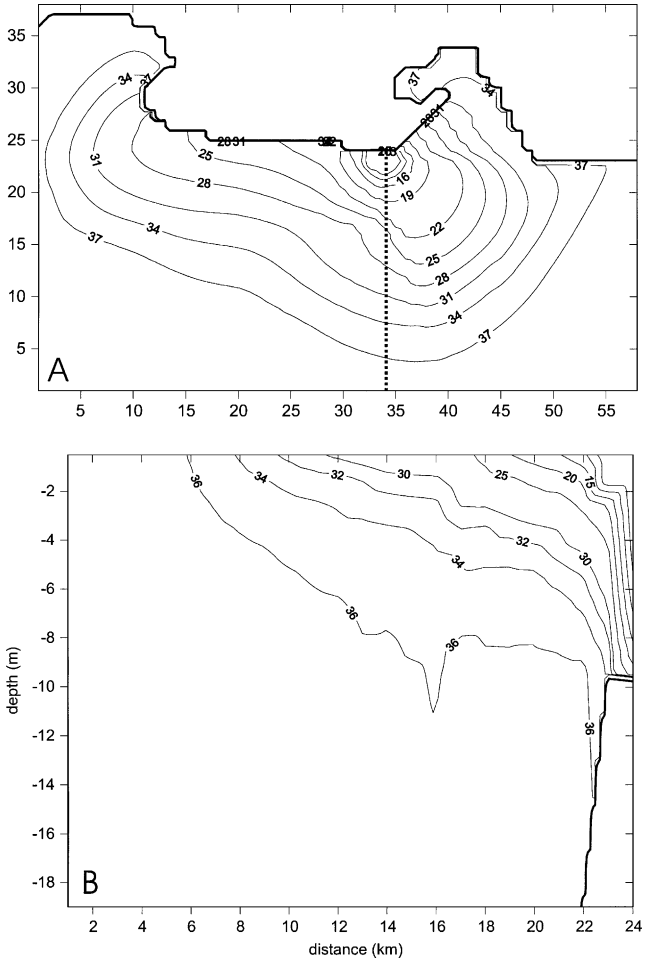

Fig. 3. A: Computed surface salinity (g/L) after a simulation time of 48 h. B: Computed salinity (g/L) south–north profile (dashed line in A) in front of the river mouth (located 24 km north from the south of the model domain) after a simulation time of 48 h.

A vertical salinity profile following a north–south line in front of the river mouth (indicated in Fig. 3A) is shown in Fig. 3B. It can be seen that the freshwater discharge is diluted with seawater due to turbulence and upwelling movements, which produce the thinning of the plume that can be appreciated in Fig. 3B. This is in agreement with the earlier computations in Marsaleix et al. (1998).

A map showing the total concentration of particles obtained after a computation time of three days can be seen in Fig. 4. Measured particle concentrations, from Martin and Thomas (1990) and Naudin et al. (2001), are also shown in Fig. 4. As commented before, the particle input from the Rhone depends on the river discharge. Sampling was carried out at different times, thus measured particle concentrations correspond to different source terms. Particle input in the model was estimated from a correlation for the particle concentration in the river mouth vs. river discharge applied to the average discharge. As a consequence, measured

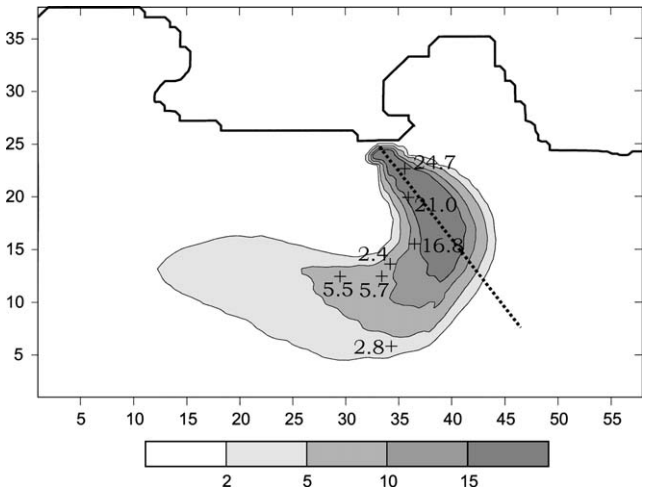

Fig. 4. Computed total suspended matter concentrations (mg/L) over the model domain at the surface after a computation time of three days and measured concentrations. The axis of the plume is also shown (dashed line).

concentrations in the plume have been normalized to a mouth particle concentration equal to 28 mg/L (source term in the model) to allow comparisons between measured and computed concentrations to be carried out. Measured concentrations presented in Fig. 4 are such normalized values.

The shape and extension of the plume is also in qualitative agreement with that obtained from satellite observations (Kondrachoff et al., 1994). It is directed to the southwest offshore, following the water circulation, and is mainly composed of fine sediments, as the coarser fractions sink close to the river mouth. This can be clearly seen with the help of Fig. 5, where the computed suspended matter concentrations at the surface for each particle class along the axis of the plume normalized to

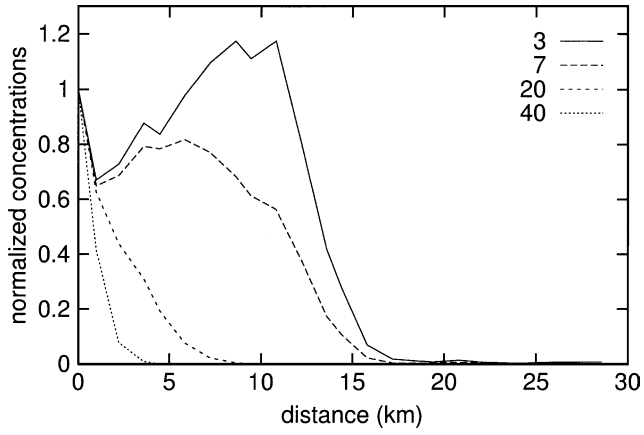

Fig. 5. Computed surface suspended matter concentrations for each particle class along the axis of the plume (dashed line in Fig. 4) normalized to the concentrations in the river mouth. Particle sizes are given in μm. Distances are measured with respect to the river mouth.

the concentrations in the river mouth are shown. Coarse particles (20 and 40 μm) soon disappear from the water column as they sink to the sea bed. The largest particles are entirely removed from the water column in less than 5 km, as found by the observations in Thill et al. (2001). The content in particles with average size 7 μm decreases to 50% in 10 km, which is similar to the distance of 8 km found in Thill et al. (2001). It can be observed that the content in the smallest particles (3 μm) initially increases, before being finally reduced as the plume is diluted. This increase in surface concentrations of the smallest particles has also been observed in Thill et al. (2001). Several hypotheses were proposed to explain it, like larger particle break-up, primary production, colloid aggregation or simple mixing with a particle-rich saline water source, although none of these mechanisms could clearly explain the behaviour of the smallest particles. It seems, however, that the particle increase is a hydrodynamic effect (particles are concentrated by the water currents some km off the river mouth) since any other process has not been included in the model.

Four maps, showing the concentration of particles for each class at the surface, are presented in Fig. 6. It can also be clearly seen how the plume is mainly composed of small particles. The two largest classes settle close to the river mouth.

The computed sedimentation rates along the plume axis (Fig. 4, dashed line) are shown in Fig. 7A together with the estimations presented in Radakovitch et al. (1999) obtained from ^{210}Pb profiles. The model underestimates the sedimentation rates. However, the following points have to be considered: first, sedimentation rates estimated from observations are maximum possible values since they are calculated assuming that there is no diffusion in the sediment core. Second, the values obtained from the model are calculated for an average water discharge, and sedimentation increases after flood events when a larger amount of suspended matter is discharged by the river. Finally, if must be taken into account that bed-load transport of coarse material is not included in the model. This process can also contribute to a larger sedimentation rate. Nevertheless, the model gives a realistic representation of the sedimentation process in the plume. Indeed, computed sedimentation rates are similar to those derived by several authors from observations (Radakovitch et al., 1999; Zuo et al., 1997; Charmasson et al., 1998): a deposition belt is observed close to the river mouth, where sedimentation reaches values of the order of 10 cm/year, decreasing on the shelf to values of the order of 10^{-1} cm/years. Sedimentation rates suffer a further decrease to values of the order of 10^{-2} cm/year when entering the deep-water basin. A map of sedimentation rates over the model domain, together with the estimations of Radakovitch et al. (1999), can be seen in Fig. 7B.

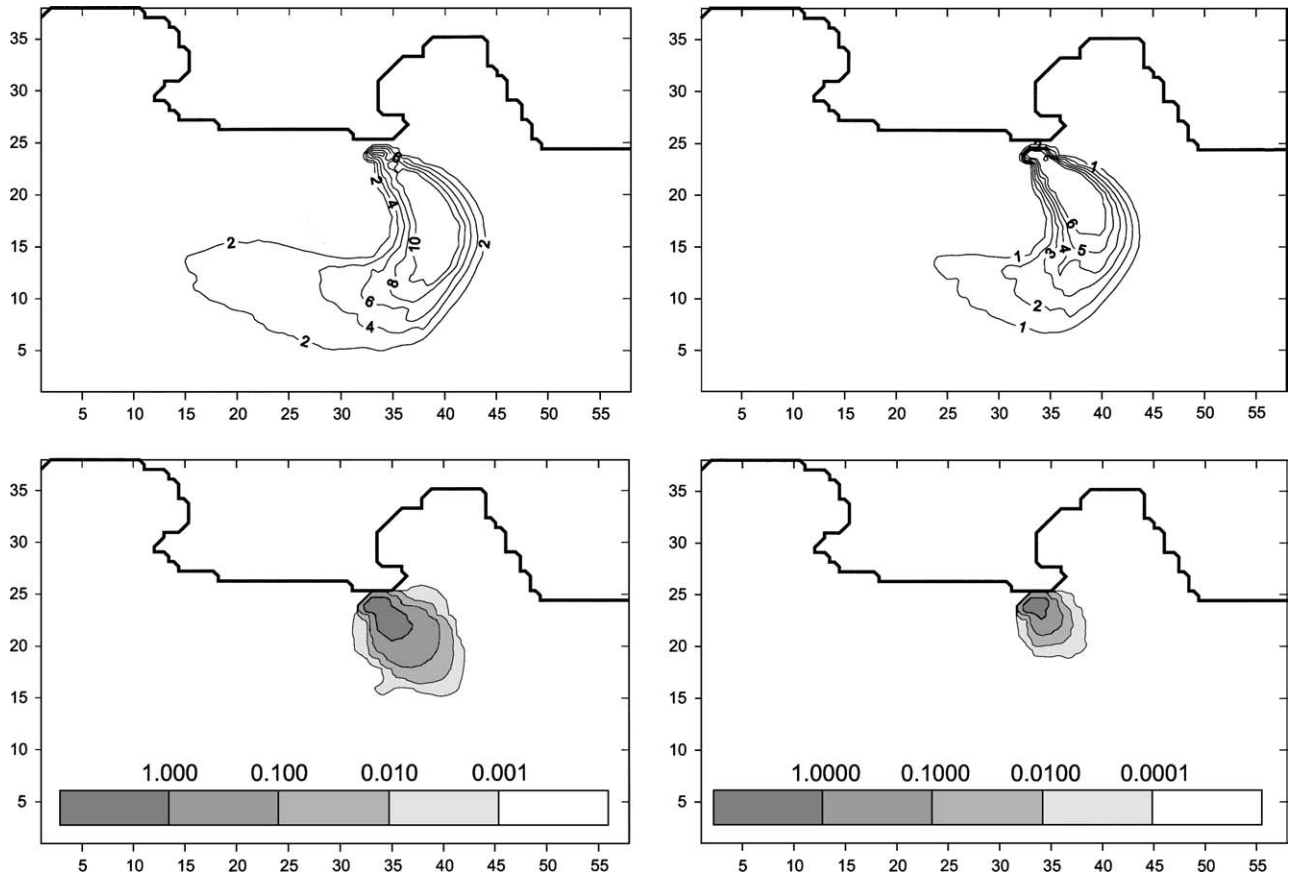

Fig. 6. Computed suspended matter concentrations at the surface for each particle class (mg/L). Left to right and top to bottom: 3, 7, 20 and 40 μm particles.

Higher values are obtained in the vicinity of the river mouth, where the coarse particles are deposited. This can also be seen in Fig. 8, where sedimentation rates for the smallest and largest particle classes are shown. Sedimentation rates are of the order of 10^{-3} g/cm^{2}year over all the model domain in the case of the 3 μm particles. However, in the case of 40 μm particles they range from 10^{-5} g/cm^2 year to 10^{-1} g/cm^2 year close to the mouth. Sedimentation rates determine the grain composition of bed sediments, which in turn is essential in the process of adsorption of dissolved contaminants. The sediment is mainly composed of the largest grain fractions, reaching 80% of 40 μm particles close to the river mouth. The fraction of 3 μm particles ranges 1–5% in most of the model domain, and it is around 7% in the case of 7 μm particles.

3.3. Dispersion of pollutants

The suspended sediment model will be applied to simulate the input of radionuclides from the Rhone River into the Mediterranean Sea. This will provide an extra validation of the suspended matter model. Radioactive pollutants have been chosen for this model application since source terms and concentrations in the plume are documented enough in current literature. Artificial radionuclides reach the Rhone River through weathering of surface soils contaminated by atmospheric fallout and through the effluents from nuclear facilities: several power plants located along the river course and, mainly, from Marcoule nuclear fuel reprocessing plant (although it was shut down in December 1997 discharges have continued since washing effluents are produced and released). The whole set of radionuclides introduced into the Rhone River will be partially exported to the Mediterranean Sea. Martin and Thomas (1990) have found that the particulate phase is the major vector for most of the radionuclides. As a consequence, any model designed to simulate the influx of radionuclides from the Rhone River into the Mediterranean Sea must consider the transport of suspended sediments and the transfers of radionuclides between the dissolved and solid phases.

The exchanges of radionuclides between the dissolved and solid phases are described in terms of kinetic transfer coefficients. Thus, assuming that adsorption/release reactions are governed by a single reversible reaction, a coefficient k_1 governs the transfer from the

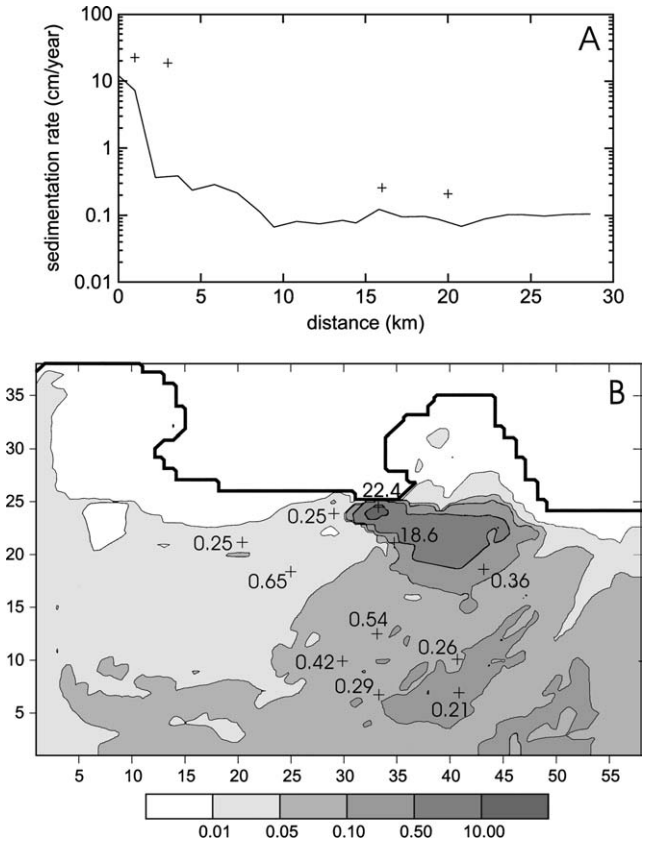

Fig. 7. A: Computed sedimentation rates along the plume axis (dashed line in Fig. 4) together with the values estimated from observations (Radakovitch et al., 1999). Distances are measured with respect to the river mouth. B: Map of computed sedimentation rates (cm/year) over the model domain and estimations from the same reference.

liquid to the solid phase and a coefficient k_2 governs the inverse process. Radionuclides in suspended matter and the dissolved phase are transported by advection/diffusion processes and those attached to the solid phase also settle with the settling velocity corresponding to the particle class to which they are fixed. They can also be deposited on the sea bed. The radionuclide dispersion model has been described before (Periáñez, 1999) in a 3D form and details will not be repeated here (although only one size of particles was considered, this does not affect the essential of the model formulation). The only difference with respect to the original model presented in Periáñez (1999) is the inclusion of the explicit dependence of the kinetic coefficient k_1 on salinity, that in this application changes from freshwater to seawater values. The coefficient k_1 depends on salinity as in Laissaoui et al. (1998):

$$k_1 = k_1^0(1-\delta) \tag{24}$$

where

$$\delta = \frac{S}{S+S_0} \tag{25}$$

In these equations k_1^0 is the freshwater value of the kinetic coefficient and S_0 is the salinity value at which 50% of saturation occurs (Laissaoui et al., 1998). It must be noted that as salinity increases, the transfer of radionuclides to the solid phase decreases due to competition effects of radionuclides with ions dissolved in water. The relations given above have been tested through laboratory experiments (Laissaoui et al., 1998).

The kinetic coefficient k_2 is considered to be constant and to have the same value for all particle classes. On the other hand, k_1 also depends on the particle size since depends on the surface of particles per water volume unit (Periáñez, 1999).

Once the water circulation, salinity distribution, suspended matter distribution for each particle class and distribution of particles in bed sediments are known and stored in files, the radionuclide dispersion model may be run using these files as input data. The radionuclide dispersion model consists of 9 equations expressing the time evolution of activity concentrations in the dissolved phase, the 4 suspended particle grain sizes and the 4 bed sediment grain sizes.

Radionuclides used in the simulations are ^{137}Cs and ^{239,240}Pu. The input of radionuclides from the river in

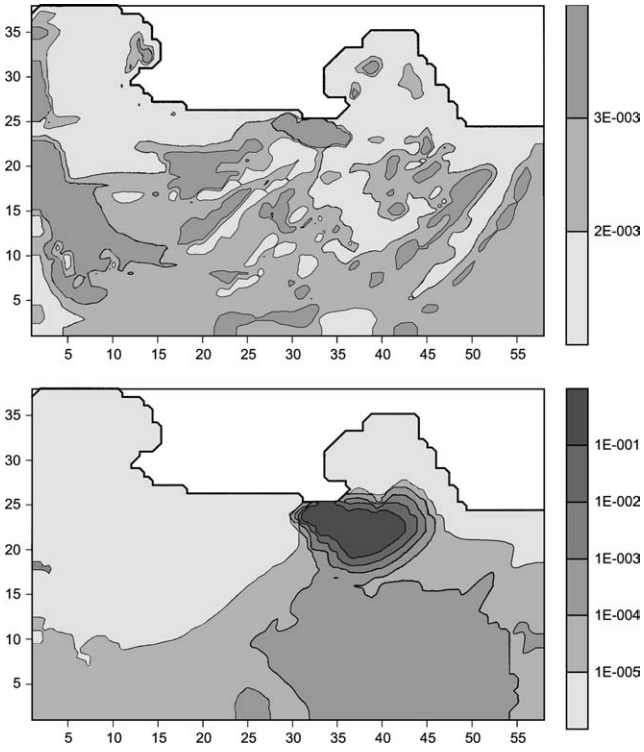

Fig. 8. Computed sedimentation rates (in g/cm^{2}year) for 3 μm (top) and 40 μm (bottom) particles.

the dissolved and particulate forms has been obtained from Martin and Thomas (1990). Inputs from the river have been obtained from sampling campaigns carried out in the period 1982–1985. For this time the main source of radionuclides to the river is the discharge from Marcoule reprocessing plant, fallout and watershed soil leaching being negligible when compared with the discharge. Also, no relevant radionuclide discharge variations have been found in these years (Martin and Thomas, 1990). Although short-term variations cannot be assessed, estimations of the inputs to the Mediterranean carried out by Martin and Thomas (1990) provide a realistic reference for the average flux of radionuclides from the Rhone. This is again justifying why winds are not used in the calculations.

Different plutonium oxidation states have not been considered in the model due to the lack of experimental data, although they could be included in the same way as in Periáñez (2003). It has also been found that Cs is not significantly fixed to colloids (Eyrolle and Charmasson 2001). The fraction of colloidal Pu measured by Eyrolle and Charmasson (2004) ranges from 0% to 41% of the dissolved phase plutonium content. Considering that over 90% of Pu is fixed to suspended matter (see below), the fraction of colloidal Pu represents a maximum of 4% of the total Pu content. Thus, colloids have been neglected in the case of Pu as well. Also, it seems that changes in POC (particulate organic carbon) content do not affect significantly the adsorption of radionuclides (Thomas, 1997).

The dispersion of radionuclides released from the river is calculated until a steady distribution is obtained. The radionuclide discharges are carried out assuming that the sea is initially not contaminated.

Model results are compared with observations in Fig. 9, where south–north profiles in front of the river mouth (see Fig. 3A) of ^{137}Cs and ^{239,240}Pu in water and suspended matter (at the surface) are shown. It can be seen that computed activity levels are, in general, in agreement with observations.

The computed distribution of ^{137}Cs in bed sediments is presented in Fig. 10, together with observations obtained from Martin and Thomas (1990). It can be seen that the model gives a correct estimation of activity levels in the vicinity of the river mouth, although underestimates them away from it. It must be taken into account that sediments integrate radionuclide input variations over time. Also, episodes of high river discharge, when larger amounts of particles are released to the sea and are also transported to greater distances from the river mouth, as well as different wind conditions, are integrated in the measured concentrations. Computed concentrations are obtained for average water, suspended particles and radionuclide discharges. It is not possible to have an accurate agreement between measurements and computations

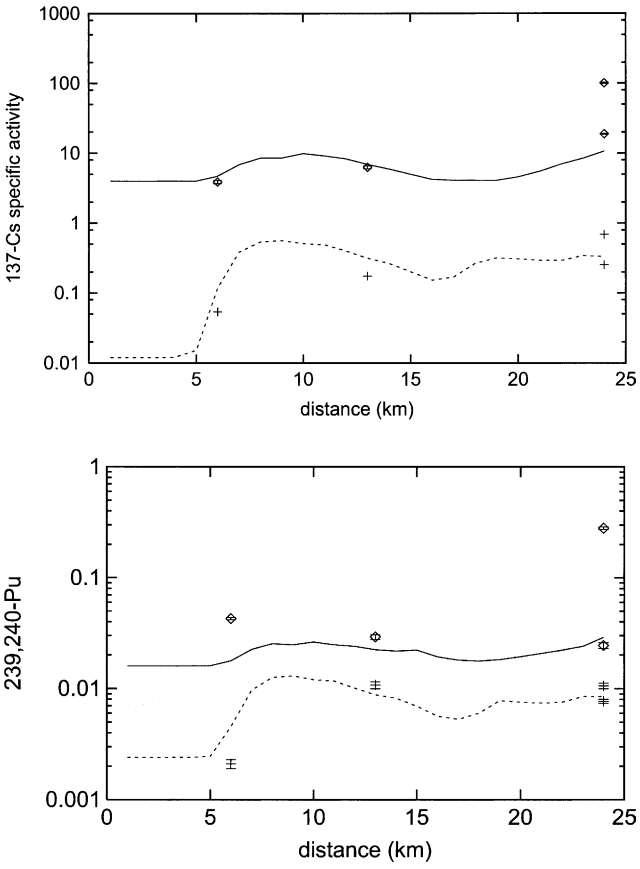

Fig. 9. Measured (points) and computed (lines) south–north profiles of ^{137}Cs and ^{239,240}Pu in surface water (solid line, boxes), Bq/m^3, and suspended matter (dashed line, crosses), Bq/g, in front of the river mouth. Distances are measured from the south of the model domain (the river mouth is at 24 km).

with a model working in *average* conditions. Nevertheless, it seems clear that the model produces rather realistic activity levels in the area of the river mouth. Indeed, the distribution map in Fig. 10 is very similar to that presented in Charmasson (2003), where a sharp decrease in inventories with distance from the river mouth can be seen. Finally, it must be taken into

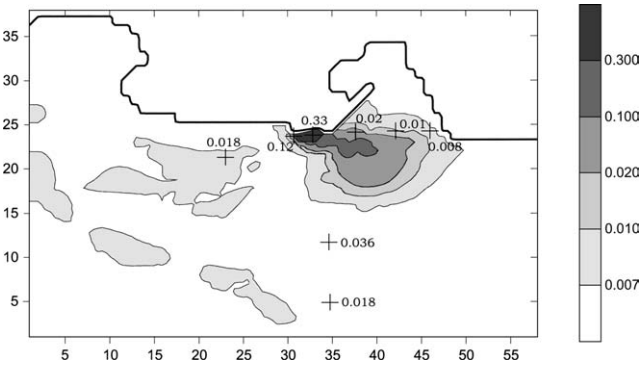

Fig. 10. Computed distribution of ^{137}Cs in bed sediments (Bq/g). Measured concentrations (Martin and Thomas, 1990) are also shown.

account that measured bed concentrations include deposition from global fallout. Only sampling stations close to the river mouth in Charmasson (2003) present ^{137}Cs inventories clearly in excess with respect to the cumulative deposit due to global fallout (Chernobyl fallout is not considered since it occurred later than the time of our simulations). Thus, most of ^{137}Cs in sediments appears in a well-delimited zone in the close vicinity of the river mouth. Our simulations are in agreement with these findings. It can also be seen that the ^{137}Cs map in sediments is directly correlated to the sedimentation rate map (Fig. 7B), indicating that the transfer of radionuclides from the water column to the sea bed is mainly due to deposition of particles, rather than to direct adsorption from the dissolved phase.

The computed fractions of ^{137}Cs and ^{239,240}Pu fixed to suspended matter particles in surface waters of the plume are presented in Fig. 11. It can be seen that about 60% of Cs is fixed to solid particles. This is in agreement with Calmet and Fernandez (1990), who found that ^{137}Cs associated with particles represents 68% of the Rhone input. The percentage increases to 90% in the case of Pu. Eyrolle and Charmasson (2004) have reported that 85% of Pu isotopes are bound to particles.

4. Conclusions

A model to simulate the transport of suspended particulate matter in the Rhone River plume has been developed. The model solves the 3D baroclinic hydrodynamic equations, including a turbulence model, together with the suspended matter equations. These include advection/diffusion, settling and deposition of particles. Four particle classes, according to observations, are considered simultaneously. The model provides suspended particle distributions and sedimentation rates for both total suspended load and each particle class. Also, it provides the distribution of particle classes over the bed sediment. Model results are, in general, in agreement with observations.

The suspended matter model has been coupled with a radionuclide dispersion model that has been used to simulate the transport of ^{137}Cs and ^{239,240}Pu in the river plume. Since the particulate phase is the major vector for the radionuclides considered, the generally good agreement between measured and computed activity levels in water, suspended matter and bottom sediments provides an extra validation of the suspended matter model. It has been calculated that over 60% of Cs and

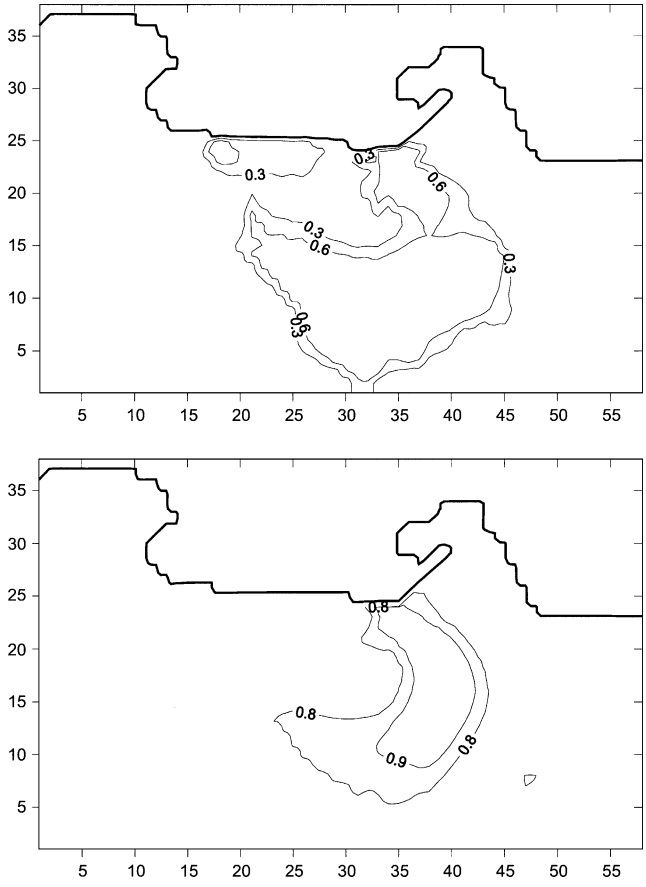

Fig. 11. Computed fractions of radionuclides fixed to suspended particles in surface waters for ^{137}Cs (up) and ^{239,240}Pu (down).

90% of Pu are fixed to suspended particles in the surface plume. Also, it has been found that activity in the plume is mainly due to the smallest particles, since the coarse ones sink rapidly to the bottom. This produces the observed deposition belt around the river mouth and the high activity levels measured in bottom sediments in this area.

Acknowledgement

This work was supported by ENRESA and EU 5th Framework Programme (1998–2002) Nuclear Fission and Radiation Protection Contract FIGE-CT-2000-00085.

References

Abril, J.M., García-León, M., 1994. Modelling the distribution of suspended matter and the sedimentation process in a marine environment. Ecological Modelling 71, 197–219.

Arnoux-Chiavassa, S., 1998. Modelisation d'ecoulements cotiers stratifies presentant des fronts: application au panache du Rhone. PhD thesis, University of Toulon.

Broche, P., Devenon, J.L., Forget, P., Maistre, J.J., Naudin, J.J., Cauwet, G., 1998. Experimental study of the Rhone plume. Part 1: physics and dynamics. Oceanologica Acta 21, 725–738.

Calmet, D., Fernandez, J.M., 1990. Caesium distribution in northwest Mediterranean seawater, suspended particles and sediments. Continental Shelf Research 10, 895–913.

Cancino, L., Neves, R., 1999. Hydrodynamic and sediment suspension modelling in estuarine systems. Part I: description of the numerical models. Journal of Marine Systems 22, 105–116.

Charmasson, S., 2003. ^{137}Cs inventory in sediment near the Rhone mouth: role played by different sources. Oceanologica Acta 26, 435–441.

Charmasson, S., Bouisset, P., Radakovitch, O., Pruchon, A.S., Arnaud, M., 1998. Long core profiles of ^{137}Cs, ^{134}Cs, ^{60}Co and ^{210}Pb in sediment near the Rhone River (northwestern Mediterranean Sea). Estuaries 21, 367–378.

Clarke, S., 1995. Advective/diffusive processes in the Firth of Forth. PhD thesis, University of Wales, Bangor, UK.

Clarke, S., Elliott, A.J., 1998. Modelling suspended sediment concentrations in the Firth of Forth. Estuarine, Coastal and Shelf Science 47, 235–250.

Cugier, P., Le Hir, P., 2002. Development of a 3D hydrodynamic model for coastal ecosystem modelling. Application to the plume of the Seine River. Estuarine, Coastal and Shelf Science 55, 673–695.

Davies, A., Hall, P., 2000. A three dimensional model of diurnal and semidiurnal tides and tidal mixing in the North Channel of the Irish Sea. Journal of Geophysical Research 105, 17079–17104.

Eisma, D., 1981. Supply and deposition of suspended matter in the North Sea. Spec. Publs Int. Ass. Sediment 5, 415–428.

Estournel, C., Kondrachoff, V., Marsaleix, P., Vehil, R., 1997. The plume of the Rhone: numerical simulation and remote sensing. Continental Shelf Research 17, 899–924.

Estournel, C., Broche, P., Marsaleix, P., Deveneon, J.L., Auclair, F., Vehil, R., 2001. The Rhone River plume in unsteady conditions: numerical and experimental results. Estuarine, Coastal and Shelf Science 53, 25–38.

Eyrolle, F., Charmasson, S., 2001. Distribution of organic carbon, selected stable elements and artificial radionuclides among dissolved, colloidal and particulate phases in the Rhone River (France): preliminary results. Journal of Environmental Radioactivity 55, 145–155.

Eyrolle, F., Charmasson, S., 2004. Importance of colloids in the transport within the dissolved phase (<450 nm) of artificial radionuclides from the Rhone River towards the Gulf of Lions (Mediterranean Sea). Journal of Environmental Radioactivity 72, 273–286.

Eyrolle, F., Arnaud, M., Duffa, C., Renaud, P., 2002. Plutonium fluxes from the Rhone River to the Mediterranean Sea. Radioprotection Colloques 37, 87–92.

Flather, R.A., Heaps, N.S., 1975. Tidal computations for Morecambe Bay. Geophysical Journal of the Royal Astronomical Society 42, 489–517.

Garnier, J.M., Martin, J.M., Mouchel, J.M., Thomas, A.J., 1991. Surface reactivity of the Rhone suspended matter and relation with trace element sorption. Marine Chemistry 36, 267–289.

Holt, J.T., James, I.D., 1999. A simulation of the southern North Sea in comparison with measurements from the North Sea Project. Part 2: suspended particulate matter. Continental Shelf Research 19, 1617–1642.

Jiang, W., Pohlmann, T., Sundermann, J., Feng, S., 2000. A modelling study of SPM transport in the Bohai Sea. Journal of Marine Systems 24, 175–200.

Kondrachoff, V., Estournel, C., Marsaleix, P., Vehil, R., 1994. Detection of the Rhone River plume using NOAA-AVHRR data. Comparison with hydrodynamic modeling results. Oceanic Remote Sensing and Sea Ice Monitoring 2319, 73–84.

Kowalick, Z., Murty, T.S., 1993. Numerical Modelling of Ocean Dynamics. World Scientific, Singapore.

Krone, R.B., 1962. Flume Studies of the Transport of Sediment in Estuarine Shoaling Processes. Final Report to the San Francisco District US Army Corps of Engineers. University of California, Berkeley.

Laissaoui, A., Abril, J.M., Periáñez, R., García-León, M., García-Montaño, E., 1998. Determining kinetic transfer coefficients for radionuclides in estuarine waters: reference values for ^{133}Ba and effects of salinity and suspended load concentrations. Journal of Radioanalytical Nuclear Chemistry 237, 55–61.

Liu, W.C., Hsu, M.H., Kuo, A.Y., 2002a. Modelling of hydrodynamics and cohesive sediment transport in Tanshui River estuarine system, Taiwan. Marine Pollution Bulletin 44, 1076–1088.

Liu, J.T., Chao, S., Hsu, R.T., 2002b. Numerical modeling study of sediment dispersal by a river plume. Continental Shelf Research 22, 1745–1773.

Lumborg, U., Windelin, A., 2003. Hydrography and cohesive sediment modelling: application to the Romo Dyb tidal area. Journal of Marine Systems 38, 287–303.

Marsaleix, P., Estournel, C., Kondrachoff, V., Vehil, R., 1998. A numerical study of the formation of the Rhone River plume. Journal of Marine Systems 14, 99–115.

Martin, J.M., Thomas, A.J., 1990. Origins, concentrations and distributions of artificial radionuclides discharged by the Rhone River to the Mediterranean Sea. Journal of Environmental Radioactivity 11, 105–139.

McKay, W.A., Walker, M.I., 1990. Plutonium and americium behaviour in Cumbria near shore waters. Journal of Environmental Radioactivity 12, 267–283.

Mehta, A.J., 1989. On estuarine cohesive sediment suspension behaviour. Journal of Geophysical Research 94 (C10), 14303–14314.

Mehta, A.J., Partheniades, E., 1975. An investigation of the depositional properties of flocculated fine sediments. Journal of Hydraulic Research 12, 361–381.

Morris, A.W., Howarth, M.J., 1998. Bed stress induced resuspension (SERE 88/89). Continental Shelf Research 18, 1203–1213.

Naudin, J.J., Cauwet, G., Fajon, C., Oriol, L., Terzic, S., Devenon, J.L., Broche, P., 2001. Effect of mixing on microbial communities in the Rhone River plume. Journal of Marine Systems 28, 203–227.

Nicholson, J., O'Connor, B.A., 1986. Cohesive sediment transport model. Journal of Hydraulic Engineering 112, 621–640.

Orlanski, I., 1976. A simple boundary condition for unbounded hyperbolic flows. Journal of Computational Physics 21, 255–261.

Periáñez, R., 1999. Three dimensional modelling of the tidal dispersion of non conservative radionuclides in the marine environment. Application to ^{239,240}Pu dispersion in the eastern Irish Sea. Journal of Marine Systems 22, 37–51.

Periáñez, R., 2000. Modelling the tidal dispersion of ^{137}Cs and ^{239,240}Pu in the English Channel. Journal of Environmental Radioactivity 49, 259–277.

Periáñez, R., 2002. Modelling the suspended matter dynamics in a marine environment using a three dimensional σ coordinate model: application to the eastern Irish Sea. Applied Mathematical Modelling 26, 583–601.

Periáñez, R., 2003. Kinetic modelling of the dispersion of plutonium in the eastern Irish Sea: two approaches. Journal of Marine Systems 38, 259–275.

Periáñez, R., Abril, J.M., García-León, M., 1996. Modelling the suspended matter distribution in an estuarine system: application to the Odiel river in southwest Spain. Ecological Modelling 87, 169–179.

Prandle, D., Hargreaves, J.C., McManus, J.P., Campbell, A.R., Duwe, K., Lane, A., Mahnke, P., Shimwell, S., Wolf, J., 2000. Tide, wave and suspended sediment modelling on an open coast, Holderness. Coastal Engineering 41, 237–267.

Pugh, D.T., 1987. Tides, Surges and Mean Sea Level. Wiley, Chichester.

Puls, W., Sundermann, J., 1990. Simulation of suspended sediment dispersion in the North Sea. In: Cheng, R.T. (Ed.), Residual Currents and Long Term Transport. Springer-Verlag, Berlin, pp. 356–372.

Radakovitch, O., Charmasson, S., Arnaud, M., Bouisset, P., 1999. ^{210}Pb and caesium accumulation in the Rhone Delta sediments. Estuarine, Coastal and Shelf Science 48, 77–92.

REMOTRANS, 2004. Processes regulating remobilisation, bioavailability, and translocation in marine sediments. EU Project FIS5-1999-00279 Remotrans 000509, Final Report.

Ruddick, K.G., Deleersnijder, E., Luyten, P.J., Ozer, J., 1995. Haline stratification in the Rhine-Meuse freshwater plume: a three dimensional model sensitivity analysis. Continental Shelf Research 15, 1597–1630.

Segschneider, J., Sundermann, J., 1998. Simulating large scale transport of suspended matter. Journal of Marine Systems 14, 81–97.

Tattersall, G.R., Elliott, A.J., Lynn, N.M., 2003. Suspended sediment concentrations in the Tamar estuary. Estuarine, Coastal and Shelf Science 57, 679–688.

Thill, A., Moustier, S., Garnier, J.M., Estournel, C., Naudin, J.J., Bottero, J.Y., 2001. Evolution of particle size and concentration in the Rhone River mixing zone: influence of salt flocculation. Continental Shelf Research 21, 2127–2140.

Thomas, A.J., 1997. Input of artificial radionuclides to the Gulf of Lions and tracing the Rhone influence in marine surface sediments. Deep Sea Research II 44, 577–595.

Tsimplis, M.N., Proctor, R., Flather, R.A., 1995. A two-dimensional tidal model for the Mediterranean Sea. Journal of Geophysical Research 100, 223–239.

Vested, H.J., Baretta, J.W., Ekebjærg, L.C., Labrosse, A., 1996. Coupling of hydrodynamical transport and ecological models for 2D horizontal flow. Journal of Marine Systems 8, 255–267.

Wu, Y., Falconer, R.A., Uncles, R.J., 1998. Modelling of water flows and cohesive sediment fluxes in the Humber Estuary, UK. Marine Pollution Bulletin 37, 182–189.

Xing, J., Davies, A., 1999. The effect of wind direction and mixing upon the spreading of a bouyant plume in a non-tidal regime. Continental Shelf Research 19, 1437–1483.

Zuo, Z., Eisma, D., Gieles, R., Beks, J., 1997. Accumulation rates and sediment deposition in the northwestern Mediterranean. Deep Sea Research II 44, 597–609.